

## **A Small Ice Towing Tank for Conceptual Modeling Part 2: Experimental Results**

Max G. Wolf

EISBÄR Architecture + Engineering Research PC, New York, New York, USA  
ORCID iD 0009-0004-6155-1989

### **ABSTRACT**

The intent of designing and building the small ice tank described below has been to provide in-house prototyping of concept designs, and basic experiments in ice mechanics and similarity when access to a full-service tank has not been possible due to high cost and other obstacles. As this paper shows and as one might suspect, the small tank cannot compete with a full-service tank's superior functionality and precision, and at times struggles to attain even its modest repertoire. Yet with a material cost of only about \$8,000 US using standard building products, it has proven extremely useful in melding theory and practice at an introductory to intermediate level and has supported rapid iterations of prototype development including a conceptual model to the point of patenting. In Part 2 of this two-part paper, model test runs demonstrate some of the tank's capacity for preliminary studies of macroscopic ice fracture and displacement patterns, and preliminary estimates of properties such as flexural strength, elastic modulus, and characteristic length, but not resistance, propulsion, maneuvering, or cycles of ice pileup.

**KEY WORDS:** towing tank, EG/AD, model ice, sea ice

### **INTRODUCTION**

Part 2 of this paper outlines basic test methods and the typical quality of data one may expect. Evaluation is presented below primarily with reference to ITTC General Guidance and Introduction to Ice Model Testing and ITTC Recommended Procedures and Guidelines - Resistance Tests in Ice. Based on this, the tank is proposed to be suitable for preliminary studies of macroscopic ice fracture and displacement patterns, preliminary estimates of properties such as flexural strength and characteristic length, but not studies on resistance, propulsion, maneuvering, or cycles of ice pileup and collapse (Polojärvi, 2022; time 23:10).

### **TWO TEST EXAMPLES**

An example of an icebreaking bow test conducted in two-stage EG/AD level ice with mean thickness of 18 mm is shown in Fig. 1 (cantilever beam thickness range: 13 – 21 mm; 1.4 m at  $\lambda 80$ ). Prior to installation of the model on the towing carriage, the ice was tempered for 172 min. with ambient air temperature of 29.5 °C and 48% RH to achieve about 10 kPa flexural strength (Fig. 2). As the graph shows, there may be a good deal of variance in the strength of in-situ beams, and the target strength (10 kPa in this case) must be estimated quickly with a trendline, which is up to now eyeballed by hand in a lab notebook and not plotted with the precision shown in Fig. 2. The blue color coded data in Fig. 2 is from another test to provide a sense of the trendlines and variance that can be expected with this method. When there is a

concern about low precision (high variance), repeating the test can often help. Qualitatively speaking, the blue data is about as precise as this process has thus far been able to produce.



Figure 1. At left, preparing the icebreaking bow for installation on the towing carriage during in-situ testing of cantilever beams. At right, the 10 kPa target has been reached and the bow is ready for testing. 16 Jun. 2024.

As shown in Fig. 1, the adjustable towing carriage is suspended from guide rails and is moved by hand. The model speed in this case averaged about 0.175 m/s (i.e., 1.6 m traversal in 9 s), which at full-scale is about 5.6 km/hr - what the USCGC Healy is specified to maintain in 1.4 m ice.<sup>1,2</sup> Test results are shown in Fig. 3. As a second example of testing with the small tank, a rafting device proposed for pack ice habitat restoration was modeled through a number of iterations culminating in a ‘preferred embodiment’, seen undergoing testing in Fig. 4 and 5, and is described in patent application PCT/US2022/049700, which can be found on WIPO’s Patentscope. A  $\lambda_{51}$  model was also run with no qualitative difference to the  $\lambda_{80}$  results.

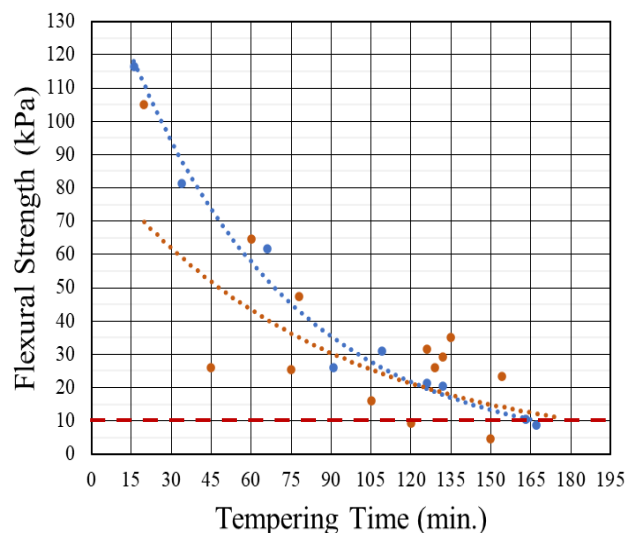


Figure 2. The slow descent to the 10 kPa target strength during tempering. Orange data points indicate in-situ beam flexural strength for the icebreaking bow test. Blue is from another test for qualitative comparison of trendlines and variance that can be expected.



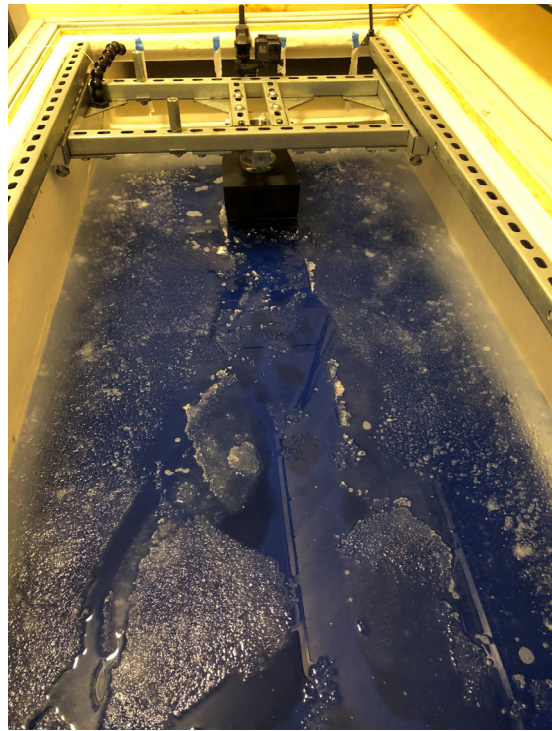


Figure 3. At left, an overhead view of test results for the icebreaking bow. Partially submerged crescent shaped fragments are visible with most having been cleared when retracting the model. At right, the undisturbed condition just after the test. There is often increased breakage adjacent to the in-situ beam test zone in the foreground. 16 Jun. 2024.

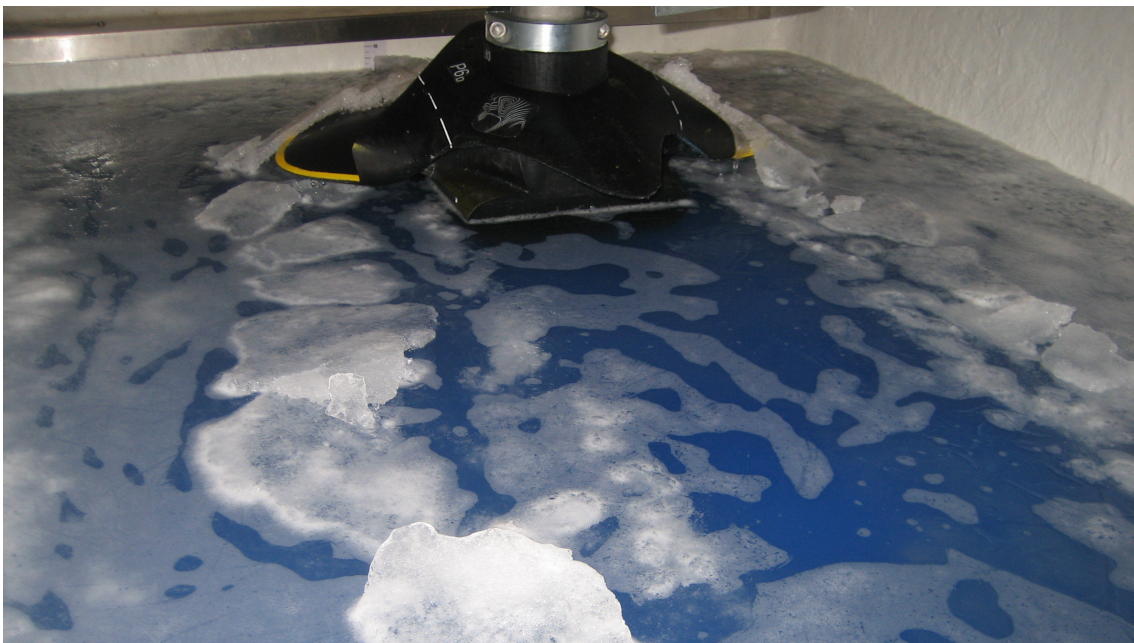


Figure 4. Ice rafting pattern at  $\lambda 80$  to verify concepts for a patent application. This is prior to finding a low suds detergent for the EG/AD ice. 11 Mar. 2021.

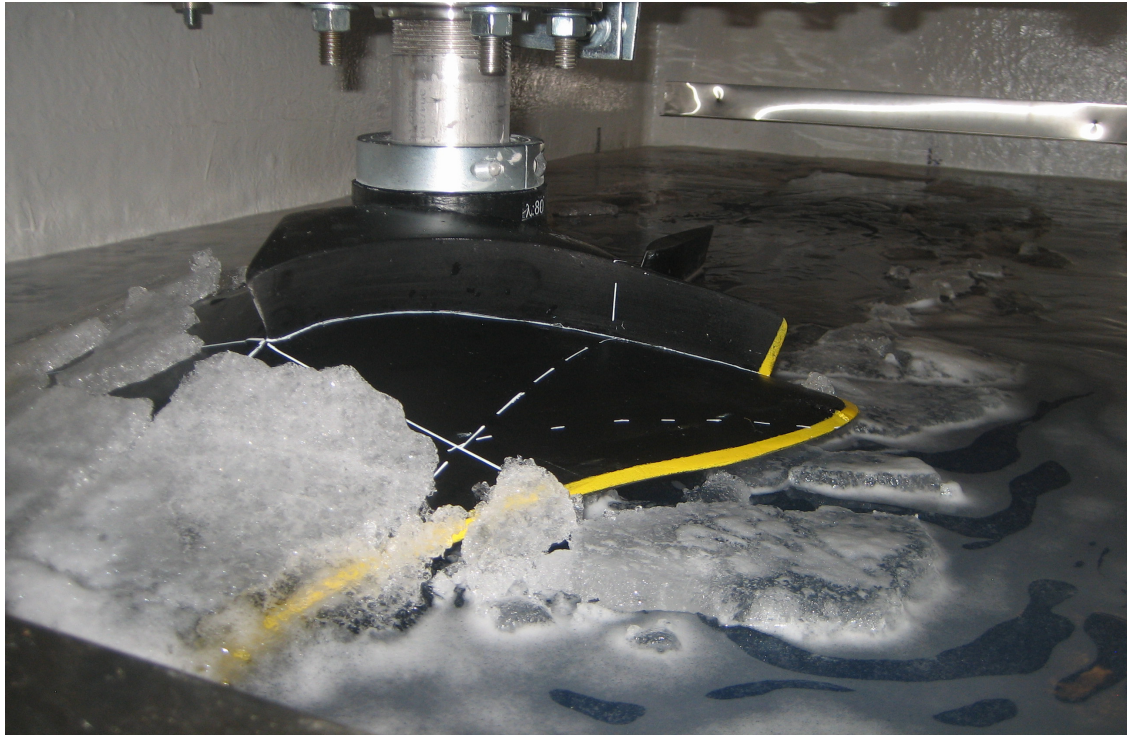


Figure 5. Front perspective of the model test run in Fig. 4.

## **SIMILARITY IN THE SMALL TANK AND ITS IMPLICATIONS**

Similarity of the model and model ice follow conventional practice based on Froude scaling of gravity and inertial forces, for example as outlined in Tatinclaux (1988). Consequently, full-scale prototype dimensions, forces and strengths are scaled down to the model by the factor  $\lambda$ , which is 80 in nearly all tests of the small ice tank due to high constraints on available space. Model ice mechanics in the small tank do not conform to Cauchy scaling, insofar as elastic similarity.

For example,  $E/\sigma_f \geq 2000$  is a typical ratio of rigidity to flexural strength found in sea ice and is generally aspired to by ice tank facilities, though it has also been questioned as ‘over rated’ (Franz von Bock und Polach & Ehlers, 2015). As an example, their calculations show that the elastic limit of the model ice in the Aalto University ice tank (fine grain ice doped with ethanol) has already been reached at a von Mises stress of less than 1 kPa, which is an order of magnitude below minimal flexural strength targets for model ice.



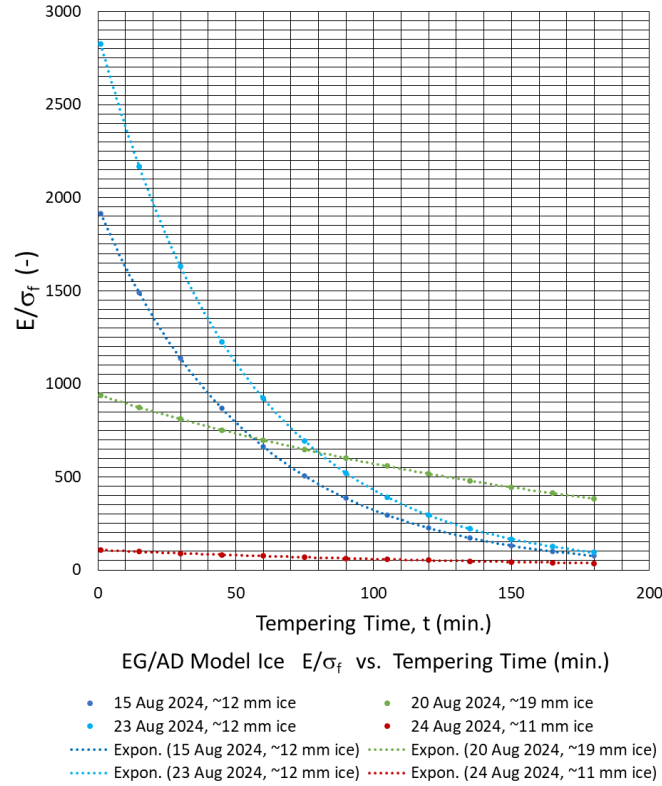


Figure 6. Examples of  $E$ -to- $\sigma_f$  ratios vs. tempering time for EG/AD second ice.

As Franz von Bock und Polach & Ehlers state, high elastic moduli can be difficult to achieve with many types of model ice.<sup>3</sup> This appears to be the case for the two-stage fine grain EG/AD ice currently used in the small ice tank (Fig. 6), though possibly for different reasons given the differences in ice chemistry, deposition method, and freezing rate. For further context, Lau et al. (2007) provide a comparison of model ice types prevalent over the last fifty years (Fig. 7), with many  $E/\sigma_f$  ratios below 2000, and two at or below 500. As seen in Fig. 6, after 120-180 minutes of tempering to achieve an estimated 10 kPa strength,  $E/\sigma_f$  can range between 50 to 500 for the two-stage EG/AD ice, which is 40 to 4 times lower than 2000.

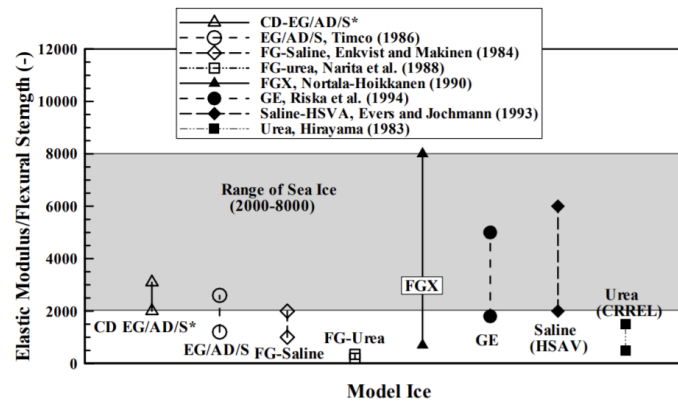


Figure 7.  $E$ -to- $\sigma_f$  ratios for prevalent model ice formulations. Image credit: Lau et al., 2007.

## Experimental Estimates of Elastic Modulus and Flexural Strength

A graph of elastic moduli vs. tempering times for the two-stage EG/AD ice tested in the small tank are shown in Fig. 8 based on Infinite Plate-Bending Method A.<sup>4</sup> Scaling up the model ice elastic moduli to full-scale by  $\lambda 80$  (column H in Table 1) yields values below 0.2 GPa as the flexural strength trendline approaches the 10 kPa target in Fig. 9.<sup>5</sup> This is far below the most flexible sea ice familiar to this author, for example, that recorded during summer in an Arctic study cited by Weeks (2010; p. 269, Fig. 10.32). The elastic modulus E in Table 1 is calculated per Method A according to:<sup>6</sup>

$$E = \frac{3}{16} \frac{(1-\nu^2)}{kh^2} (F/\delta)^2 \quad [\text{Pa}] \quad (1)$$

Where:

- F = loading force [N]
- g = acceleration of gravity [m/s<sup>2</sup>]
- k = foundation factor, where  $k = \rho_w g$  [kg/m<sup>2</sup>-s<sup>2</sup>]
- h = ice thickness [m]
- $\delta$  = vertical deflection [m]
- $\nu$  = Poisson's ratio [-]
- $\rho_w$  = EG/AD melt solution density [kg/m<sup>3</sup>]

Examples of the two-stage EG/AD ice flexural strength vs. tempering time from in-situ beam tests is shown in Fig. 9, with variance in flexural strength data similar to that of the conventionally frozen EG/AD ice tested by Kim and Choi (2011, their Fig. 2), and the fine grain EG/AD ice proposed by Ha et al (2015, their Fig. 7). Within 120-180 minutes of tempering for an average thickness of 12 mm, trendlines approach the target strength of 10 kPa.

Table 1. Sample data from Infinite Plate-Bending Method A and in-situ cantilever beam testing to estimate model ice elastic modulus (col. E) and flexural strength (col. J). Blank entries indicate a failed test. Tests were conducted on the same ice sheet on 23 Aug. 2024.

Load Test	Load Mass	Load Force	Ice Plate Deflection	Elastic Modulus	Ice Tempering Time	Ice Thickness	Scaled-up Elastic Modulus	Load Test	Measured Flexural Strength	Ice Tempering Time
A	B	C=9.81*B	D	E	F	G	H =80*E/10 <sup>6</sup>	I	J	K
	m	F = mg	$\delta$	E	t	h	( $\lambda=80$ ) x E		$\sigma_f$	t
	(kg)	(N)	(m)	(kPa)	(min)	(m)	(GPa)		(kPa)	(min)
1	0.020	0.20	0.00001	46,449	23	0.012	3.72	1	91.0	27
2	0.050	0.49	0.00002	72,576	30	0.012	5.81	2	45.3	45
3	0.050	0.49	0.00003	32,256	52	0.012	2.58	3	64.9	54
4	0.100	0.98	0.00007	23,698	58	0.012	1.90	4	44.8	67
5	0.020	0.20	0.00001	46,449	60	0.012	3.72	5	20.5	93
6	0.050	0.49	0.00005	11,612	75	0.012	0.93	6	35.7	101
7	0.040	0.39	0.00004	11,612	79	0.012	0.93	7	35.7	112
8	0.050	0.49	0.00007	5,925	92	0.012	0.47	8	20.3	113
9	0.050	0.49	0.00011	2,399	118	0.012	0.19	9	10.0	120
10	0.030	0.29	0.00006	2,903	120	0.012	0.23	10	23.5	126
11	0.050	0.49	0.00012	2,016	133	0.012	0.16	11		
12	0.020	0.20	0.00005	1,858	134	0.012	0.15	12	23.8	131
13	0.050	0.49	0.00013	1,718	145	0.012	0.14	13	18.7	135
14	0.050	0.49	0.00019	804	150	0.012	0.06	14	15.5	146
15	0.020	0.20	0.00008	726	155	0.012	0.06	15	9.6	150

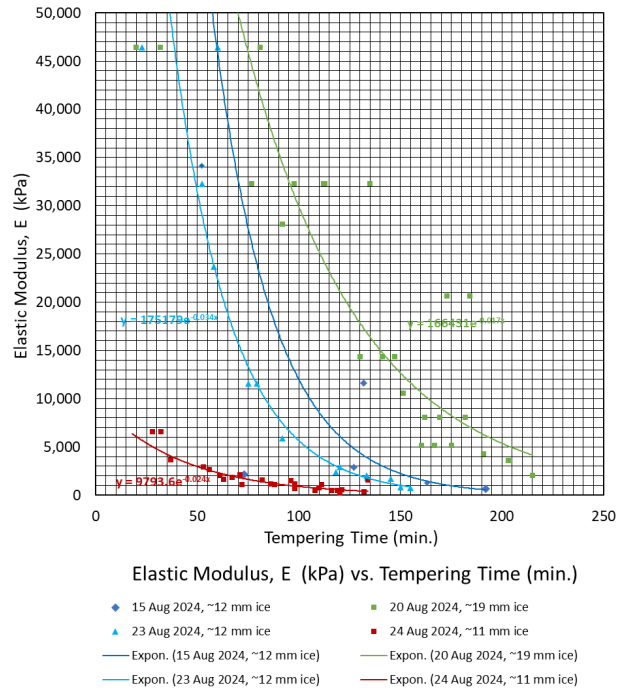


Figure 8. Examples of elastic modulus vs. tempering time for EG/AD second ice.

Horizontal rows of data points for the 19 mm ice in Fig. 8 are due to the limited precision of the vertical displacement gauge (Fig. 11) in combination with loads that are multiples of one another, e.g. (0.06 kg load / 0.00002 m displacement) at 81 minutes yields the same estimate of E as (0.03 kg / 0.00001 m displacement) at 20 and 32 minutes.

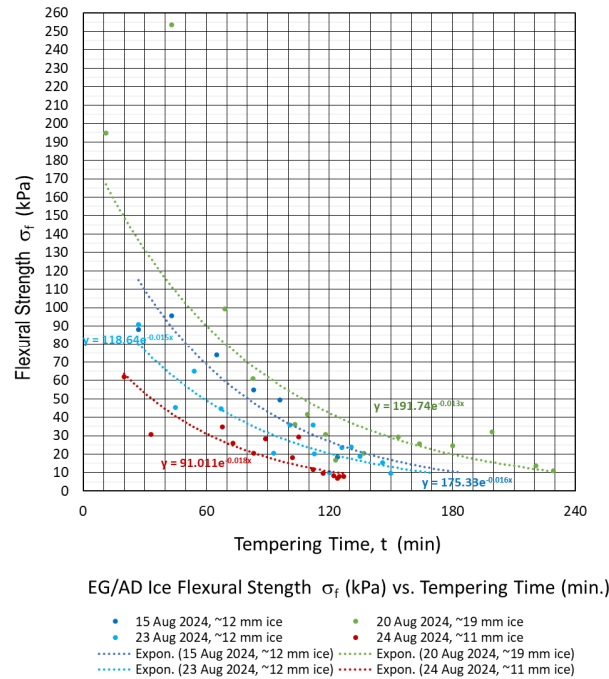


Figure 9. EG/AD second ice flexural strength vs. tempering time of in-situ beam tests.

## Methods of Measuring Model Ice Properties

Model ice flexural strength is calculated from in-situ tests of cantilever beams (Fig. 10, left) according to ITTC guidelines, and are cut with a handheld router (Bosch GKF125CE-RT 1.25 HP Variable Speed Palm Router) guided by a plywood template prior to tempering (Fig. 10, right). Routed beam dimensions are approximately 85 mm long x 40 mm wide for 10-20 mm thickness. During testing, a gradually increasing downward load is applied at beam tips with a hand-held force gauge (DST-1A by IMADA. Chatillon spring gages mentioned by Tatinclaux (1984) were found to be too stiff for 10 kPa ice). Per ITTC guidelines, flexural strength is calculated according to<sup>7</sup>:

$$\sigma_f = 6Fl_b/bh^2 \quad [\text{Pa}] \quad (2)$$

Not enough data has been gathered to estimate any difference in strength between downward and upward loading for the EG/AD second ice.

Elastic modulus is estimated with the Infinite Plate-Bending Method A using a displacement gauge (Mitutoyo Digimatic 543-705B) fitted with a PLA plastic contact to reduce thermal conductance and local surface damage (Fig. 11, left). A pre-cooled mass conforming to ASTM F1 tolerance loads the ice sheet as the gauge indicates deflection within a 2-3 second limit to minimize the contribution of creep. Corresponding ice thicknesses around the sheet are measured in parallel to deflection testing with small bore holes (Fig. 11, right).



Figure 10. At left, measurement of flexural strength with cantilever beams using a DST-1A force gauge. At right, cutting of cantilever beams in an untempered ice sheet with plywood guide. (A wider diameter bit to reduce stress risers at cantilever roots is being developed.)

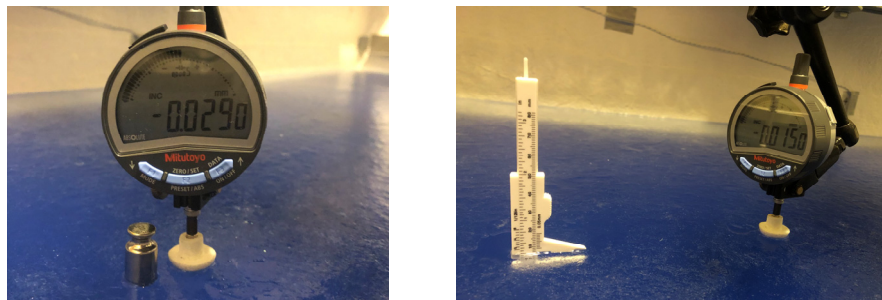


Figure 11. At left, measurement of elastic modulus with displacement gauge and 20 g mass. At right, measurement of model ice sheet thickness with a plastic (low thermal conductivity) caliper through a 25 mm diameter borehole near the displacement gauge.

## DISCUSSION AND CONCLUSIONS



Concerns remaining for the small tank and two-stage EG/AD ice are the persistently low  $E/\sigma_f$  ratios and a characteristic length that is too short compared to full-scale sea ice. Nevertheless, fracture and displacement patterns appear credible when measured and compared to similar full-scale situations. Enlarging and improving insulation of the basin, increasing freezer unit power, and providing a symmetric layout of air convection may help (Fig. 12). An extended basin length of about 7-8 m would just begin to allow for preliminary resistance testing of a conventional icebreaker at  $\lambda_{80}$ , i.e., two vessel lengths ( $\sim 1.6 \text{ m} \times 2$ ) into the ice followed by two lengths or more of resistance data. Finally, working with 12 mm two-stage EG/AD ice down to 10 kPa can be challenging due to fragility, which can make some measurements at the end of tempering questionable, so slightly thicker ice or ice around 15 kPa is recommended when constraints allow.

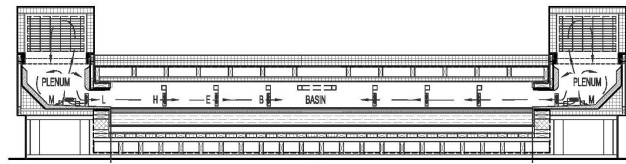


Figure 12. Concept for a second ice tank with extended basin length and 1.5 m width.

## ACKNOWLEDGEMENTS

Development of the small ice tank and this paper have been self-funded. The paper is based on a confidential unpublished report by this author to provide validation of testing for an ice rafting device as described in the patent application noted in Part 2, and as part of a master of engineering thesis detailing its prototyping. The author gratefully acknowledges the expertise of Lucas Kriz, Director of Research and Development at Central Solutions, Kansas City, KS in the selection of a suitable low suds aliphatic detergent and for a sample donated for use. The author also thanks Prof. R.U. Franz von Bock und Polach, Technische Universität Hamburg, for encouragement and preliminary review of the confidential report. None of this is to be construed as endorsement of the tank or this paper, any errors being entirely mine.

## REFERENCES

- Daley, C., 2010. Sea Ice Engineering, theory and application. *Lecture note for EN8674/9096, Memorial University of Newfoundland*, pp.5-30.
- Franz von Bock und Polach, R.U. and Ehlers, S., 2015. On the scalability of model-scale ice experiments. *Journal of offshore mechanics and arctic engineering*, 137(5), p.051502.
- Ha, J.S., Cho, S.R., Jeong, S.Y., Yeom, J.G. and Kang, K.J., 2015. An Experimental Study and a New Method Used to Prepare Granular EG/AD Model Ice. In *Proceedings of the International Conference on Port and Ocean Engineering Under Arctic Conditions*.
- Hetényi, M., & Hetbenyi, M. I., 1971. *Beams on elastic foundation: theory with applications in the fields of civil and mechanical engineering* (Vol. 16). Ann Arbor, MI: University of Michigan press.

- ITTC., 2017. Test Methods for Model Ice Properties. 7.5-02-04-02. Revision 2. International Towing Tank Conference. <https://www.ittc.info/media/8061/75-02-04-02.pdf>.
- Kim, J.H. and Choi, K.S., 2011. Comparison of EG/AD/S and EG/AD model ice properties. *International Journal of Ocean System Engineering*, 1(1), pp.32-36.
- Lau, M., Wang, J. and Lee, C., 2007. Review of ice modeling methodology. In *Proceedings of the International Conference on Port and Ocean Engineering Under Arctic Conditions*.
- Michel, B., Ice mechanics, 1978. *Les Presses de l'Université Laval. Québec*.
- Polojärvi, A., 2022. “Dr. Polojärvi - Presentation at the Isaac Newton Institute”. YouTube, Uploaded by INI Seminar Room 1 10 April, 2022, <https://www.youtube.com/watch?v=8RV5ikLtGeE> Accessed 14 July 2024.
- Pratte, B.D. and Timco, G.W., 1981. A new model basin for the testing of ice-structure interactions. Proc. POAC 81, Quebec City, Canada, Vol. II, pp. 857-866.
- Tatinclaux, J.C., 1989. *Model Tests in Ice of a Canadian Coast Guard R-class Icebreaker-high Friction Model* (Vol. 89, No. 25). US Army Corps of Engineers Cold Regions Research & Engineering Laboratory.
- Tatinclaux, J. C., 1988. Ship model testing in level ice: an overview.
- Timco, G.W., 1986. EG/AD/S: A new type of model ice for refrigerated towing tanks. *Cold Regions Science and Technology*, 12(2), pp.175-195.
- Weeks, W., 2010. *On sea ice*. University of Alaska Press.

## ENDNOTES

<sup>1</sup> As required by Froude scaling, the ratio of prototype to model velocities is proportional to the square root of the length scale:  $V_p/V_m = \lambda^{1/2} = 80^{1/2} = 8.94$ . Assuming a speed of 5.6 km/hr in 1 meter ice:  $V_m = V_p/8.94 = 5.6 \text{ km/hr}/8.94 = 0.63 \text{ km/hr}$  model speed = 0.175 m/s or 5.7 s/m;  $5.7 \text{ s/m} * 1.6 \text{ m} = 9.1 \text{ s}$ .

<sup>2</sup> [https://en.wikipedia.org/wiki/USCGC\\_Healy](https://en.wikipedia.org/wiki/USCGC_Healy)

<sup>3</sup> Franz von Bock und Polach (2015): “Based on Froude scaling dimensionless ratios in model-scale and full-scale must be equal. Schwarz (1985) postulated that the ratio  $E/\sigma_f$  (Elastic modulus / flexural strength) should be equal in model-scale and full-scale and represent a quality measure. In full-scale the ratio is considered to express the brittleness of the ice and lies well above 2000. In model-scale this ratio is not often reached, but lower to a ratio of 1000 (see Schwarz 1977). At Aalto Ice Tank those ratios are usually 900 – 2500.”

<sup>4</sup> Section 3.1.1 of ITTC Test Methods for Model Ice Properties 7.5-02-04-02 (2014) Rev 02.

<sup>5</sup> 10 kPa target flexural strength is based on 800 kPa full-scale assumption - hard winter ice.

<sup>6</sup> Infinite Plate-Bending Method A, ITTC 7.5-02-04-02, 2014, Rev 02 - Test Methods for Model Ice Properties. <https://www.ittc.info/media/8061/75-02-04-02.pdf>

<sup>7</sup> Eqn. 1, ITTC 7.5-02-04-02, 2014, Rev 02.